

Penalized Matrix Regression for Two-Dimensional Variable Selection

Cheoljoon Jeong and Xiaolei Fang
 Edwards P. Fitts Department of Industrial and Systems Engineering
 North Carolina State University

September 20, 2019

Abstract. The root-cause diagnostics for product quality defects in multistage manufacturing processes often requires us to simultaneously identify the crucial stages and variables. To satisfy this requirement, this paper proposes a novel penalized matrix regression methodology for two-dimensional variable selection. The method regresses a matrix-based predictor against a scalar-based response variable using a generalized linear model. The rows and columns of the regression coefficient matrix are simultaneously penalized to inspire sparsity. To estimate the parameters, we develop a block coordinate proximal descent (BCPD) optimization algorithm, which cyclically solves two sub optimization problems, both of which have closed-form solutions. A simulation study and data from a real-world application are used to validate the effectiveness of the proposed method.

Keywords. Penalized matrix regression, Two-dimensional variable selection, Adaptive Group Lasso, Block Coordinate Proximal Descent

1 Introduction

Multistage manufacturing is a complex process that consists of multiple components, stations or stages to produce a product. For instance, Figure 1 illustrates a seven-stage hot strip mill, the primary function of which is to roll heated steel slabs thinner and longer through 7 successive rolling mill stands and coil up the lengthened steel sheet for transport to the next process. The advancements in sensing technology and data acquisition systems have facilitated us to collect massive amount of control and sensor data during the operation of such multistage processes. If modeled properly, these data could be very useful for system performance monitoring and diagnostics. System monitoring focuses on detecting defects/anomalies in real-time and diagnostics aims at identifying the root-cause of the detected defects. One of the most important types of defect in manufacturing is a product quality defect. Diagnostics for product quality defects in multistage manufacturing processes is challenging since multistage manufacturing processes typically consist of many stages, which involve a large amount of control and sensor data (referred to as “process variables” hereafter). Figure 2 shows some examples of process variables from the hot strip mill mentioned earlier. This paper focuses on the product quality defect diagnostics of multistage manufacturing processes that all stages have similar operations, such as the one illustrated in Figure 1.

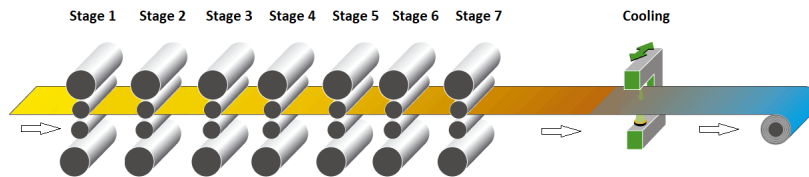


Figure 1: A hot strip mill with seven stands.

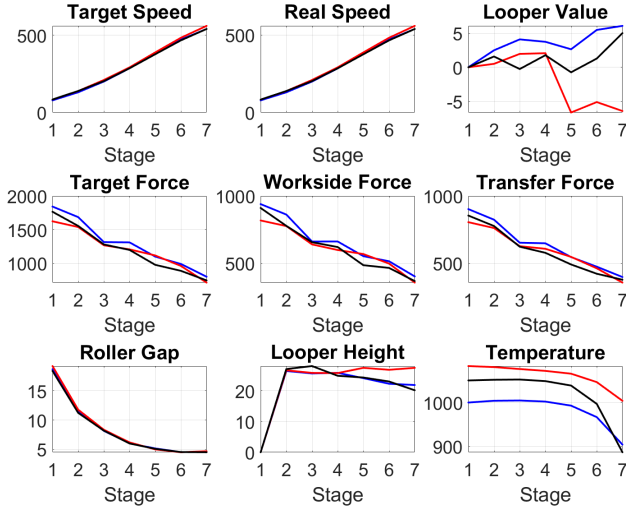


Figure 2: Process variables for the hot strip mill.

A straightforward method for product quality defect diagnostics is LASSO [4], which regresses quality index against process variables and penalizes the regression coefficients to inspire sparsity. Any process variable with a nonzero coefficient is considered to be responsible for quality defects. However, one of the limitations of LASSO is that it cannot provide a structured solution that people can use to revise the control model of a multistage manufacturing process to avoid further quality defects. To be specific, due to the correlation among process variables, it is expected that LASSO selects various process variables at different stages, which are difficult to be used to guide control model revision. In reality, engineers are interested in identifying a few crucial process variables as well as stages that significantly affect product quality. For example, Table 1 shows a process variable matrix, the rows of which are process variables and columns represent stages. The cross markers represent the non-crucial process variables and stages for quality defect diagnostics. For the multistage manufacturing process illustrated in Table 1, engineers expect that process variables 1, 4 and stages 1, 3 can be respectively identified as crucial process variables and stages. To achieve this goal, one possible solution is to use group LASSO [9] to penalize the rows to identify crucial process variables, and then remove the identified non-crucial rows and apply group LASSO again on the columns to select important stages. However, an obvious limitation of doing this is that the row selection is negatively affected by the non-crucial columns. Consequently, the selection accuracy is compromised.

	Stage 1	Stage 2	Stage 3	Stage 4
Process variable 1		×		×
Process variable 2	×	×	×	×
Process variable 3	×	×	×	×
Process variable 4		×		×
Process variable 5	×	×	×	×

Table 1: An example process variable matrix (the cross markers represent the non-crucial process variables and stages).

To address this challenge, this paper proposes a 2D variable selection methodology, which is capable of simultaneously identifying the crucial process variables and stages that are responsible for product quality defects. This is achieved by developing a penalized matrix regression model that regresses a product’s quality index against its process variable matrix. The quality index is assumed to be from an exponential family distribution (i.e., normal, binomial, Poisson, gamma, exponential, etc.). Identifying the crucial process variables and stages is equivalent to jointly selecting the important rows and columns of the process variable matrix. To do this, we decompose the unknown regression coefficient matrix as a product of two factor matrices. We then penalize the rows of the first factor matrix and columns of the second factor matrix using group LASSO. The joint penalization on the two factor matrices results in both row-wise and column-wise sparsity on their product matrix (aka. the regression coefficient matrix). To estimate the regression coefficient matrix, we develop a block coordinate proximal descent (BCPD) algorithm, which cyclically optimizes one of the two factor matrices until convergence. We have proved that each step of the proposed BCPD algorithm achieves a closed-form solution, which helps significantly speed up the parameter estimation process.

The rest of this paper is organized as follows. In Section 2, we introduce the 2D variable selection methodology. Section 3 presents the optimization algorithm. Sections 4 and 5 validate the performance of our proposed 2D variable selection method using a numerical study and a real-world dataset, respectively. Finally, Section 6 concludes.

2 2D Variable Selection Methodology

This paper proposes a 2D variable selection methodology, which jointly identifies the crucial process variables and stages that are responsible for quality defects of a multistage manufacturing process. This is achieved by developing a generalized matrix regression model with regularization.

We assume that there exists a historical dataset for model training (aka. parameter estimation). The dataset consists of the quality index and process variables of n products from the same multistage manufacturing process. We denote the quality index and process variable matrix of product i as y_i and $\mathbf{X}_i \in \mathbb{R}^{s \times t}$, respectively, where s is the number of process variables and t is the number of stages. As pointed out earlier, we assume that y_i is from an exponential family distribution. Therefore, its probability mass or density function can be expressed as follows:

$$\mathbb{P}(y_i|\theta_i, \phi) = \exp \left\{ \frac{y_i\theta_i - b(\theta_i)}{a(\phi)} + c(y_i, \phi) \right\}, \quad (1)$$

where θ_i and $\phi > 0$ are parameters. Generalized matrix regression can be built by relating the process variable matrix \mathbf{X}_i to the mean $\mu_i = \mathbb{E}(y_i|\mathbf{X}_i)$ via the model below:

$$g(\mu_i) = b + \langle \mathbf{B}, \mathbf{X}_i \rangle, \quad (2)$$

where $\mathbf{B} \in \mathbb{R}^{s \times t}$ is the regression coefficient matrix. b is the intercept. $\langle \cdot \rangle$ is the matrix inner product operator, which is defined as $\langle \mathbf{B}, \mathbf{X}_i \rangle = \langle \text{vec}(\mathbf{B}), \text{vec}(\mathbf{X}_i) \rangle$. The coefficient of the above generalized matrix regression can be estimated by using maximum likelihood estimation (MLE) method, which maximizes the following log-likelihood function:

$$\ell(\mathbf{B}, b) = \sum_{i=1}^n \frac{y_i\theta_i - b(\theta_i)}{a(\phi)} + \sum_{i=1}^n c(y_i, \phi), \quad (3)$$

where θ_i is related to regression parameters (\mathbf{B}, b) . We denote a loss function by $\mathcal{L}(\cdot)$, which is a negative log-likelihood function $\ell(\cdot)$. Then, we can minimize $\mathcal{L}(\cdot)$ to estimate parameters as follows:

$$\min_{\mathbf{B}, b} \mathcal{L}(\mathbf{B}, b) = \max_{\mathbf{B}, b} \ell(\mathbf{B}, b). \quad (4)$$

To achieve both row-wise and column-wise selection, we decompose the unknown regression coefficient matrix as a product of two factor matrices: $\mathbf{B} = \mathbf{U}\mathbf{V}$, where $\mathbf{U} \in \mathbb{R}^{s \times r}$, $\mathbf{V} \in \mathbb{R}^{r \times t}$, and r is the unknown rank that will be selected using AIC. As a result, the link function in Equation (2) can be expressed as follows:

$$g(\mu_i) = b + \langle \mathbf{U}\mathbf{V}, \mathbf{X}_i \rangle. \quad (5)$$

We then penalize the rows of \mathbf{U} and columns of \mathbf{V} respectively using adaptive group LASSO, which results in the following optimization criterion:

$$\min_{\mathbf{U}, \mathbf{V}, b} \mathcal{L}(\mathbf{U}, \mathbf{V}, b) + \mathcal{R}(\mathbf{U}, \mathbf{V}), \quad (6)$$

where the regularization term

$$\mathcal{R}(\mathbf{U}, \mathbf{V}) = \lambda\gamma \left(\sum_{j=1}^s \frac{\|\mathbf{u}_j\|_2}{\|\hat{\mathbf{u}}_j\|_2} + \sum_{k=1}^t \frac{\|\mathbf{v}_k\|_2}{\|\hat{\mathbf{v}}_k\|_2} \right). \quad (7)$$

Here, $\lambda \geq 0$ is the tuning parameter. $\|\cdot\|_2$ is ℓ_2 norm. $\gamma = \sqrt{r}$, which is used to rescale the penalty with respect to the length of \mathbf{u}_j and \mathbf{v}_k (aka. group LASSO). $\mathbf{u}_j \in \mathbb{R}^r$ is the j th row of matrix \mathbf{U} and $\mathbf{v}_k \in \mathbb{R}^r$ is the k th column of matrix \mathbf{V} . $\hat{\mathbf{u}}_j$ and $\hat{\mathbf{v}}_k$ are the regular maximum likelihood estimates of \mathbf{u}_j and \mathbf{v}_k , respectively. They are also used to scale the penalized coefficients (aka. adaptive group LASSO), which help address the estimation inefficiency and selection inconsistency challenges in group LASSO penalization.

Solving optimization criterion (6) provides factor matrices $\hat{\mathbf{U}}$ and $\hat{\mathbf{V}}$ with sparse rows and columns, respectively. Consequently, the estimated regression coefficient matrix $\hat{\mathbf{B}} = \hat{\mathbf{U}}\hat{\mathbf{V}}$ has both sparse rows and columns. The process variables corresponding to the nonzero rows and the stages corresponding to the nonzero columns are considered crucial for product quality defects.

3 Optimization Algorithm

In this section, we develop a block coordinate proximal descent (BCPD) algorithm to solve optimization criterion (6). Before introducing BCPD, we first introduce a simple optimization algorithm based on block coordinate descent (BCD), which is also able to solve optimization criterion (6).

3.1 Block Coordinate Descent

BCD iteratively updates (\mathbf{U}, b) with \mathbf{V} fixed and then (\mathbf{V}, b) with \mathbf{U} fixed. Mathematically, it is achieved by solving the following two subproblems iteratively:

$$(\mathbf{U}^k, \hat{b}^k) = \underset{\mathbf{U}, b}{\operatorname{argmin}} \mathcal{L}(\mathbf{U}, \mathbf{V}^{k-1}, b) + \mathcal{R}(\mathbf{U}, \mathbf{V}^{k-1}), \quad (8)$$

$$(\mathbf{V}^k, b^k) = \underset{\mathbf{V}, b}{\operatorname{argmin}} \mathcal{L}(\mathbf{U}^k, \mathbf{V}, \hat{b}^k) + \mathcal{R}(\mathbf{U}^k, \mathbf{V}). \quad (9)$$

We summarize the BCD algorithm in the table below.

Algorithm Block Coordinate Descent

Input: $\{\mathbf{X}_i, y_i\}_{i=1}^n$

Initialization: Randomly choose $(\mathbf{U}^0, \mathbf{V}^0, b^0)$

while convergence criterion not met **do**

 Compute $(\mathbf{U}^k, \hat{b}^k)$ using (8)

 Compute (\mathbf{V}^k, b^k) using (9)

 Let $k = k + 1$

end while

Both optimization problems (8) and (9) are convex and thus can be solved using many existing algorithms and packages such as CVX and CVXQUAD [3]. However, existing convex optimization algorithms for solving (8) and (9) are computationally intensive, and thus are not suitable for applications with large-size data.

3.2 Block Coordinate Proximal Descent

To accelerate the computation speed, we propose a BCPD algorithm. To be specific, at iteration k , we solve the following subproblems:

$$\mathbf{U}^k = \underset{\mathbf{U}}{\operatorname{argmin}} \langle \nabla_{\mathbf{U}} \mathcal{L}(\mathbf{U}^{k-1}, \mathbf{V}^{k-1}, b^{k-1}), \mathbf{U} - \mathbf{U}^{k-1} \rangle + \frac{L_u^k}{2} \|\mathbf{U} - \mathbf{U}^{k-1}\|_F^2 + \mathcal{R}(\mathbf{U}, \mathbf{V}^{k-1}), \quad (10)$$

$$\hat{b}^k = \underset{b}{\operatorname{argmin}} \langle \nabla_b \mathcal{L}(\mathbf{U}^{k-1}, \mathbf{V}^{k-1}, b^{k-1}), b - b^{k-1} \rangle + \frac{L_u^k}{2} (b - b^{k-1})^2, \quad (11)$$

$$\mathbf{V}^k = \underset{\mathbf{V}}{\operatorname{argmin}} \langle \nabla_{\mathbf{V}} \mathcal{L}(\mathbf{U}^k, \mathbf{V}^{k-1}, \hat{b}^k), \mathbf{V} - \mathbf{V}^{k-1} \rangle + \frac{L_v^k}{2} \|\mathbf{V} - \mathbf{V}^{k-1}\|_F^2 + \mathcal{R}(\mathbf{U}^k, \mathbf{V}), \quad (12)$$

$$b^k = \underset{b}{\operatorname{argmin}} \langle \nabla_b \mathcal{L}(\mathbf{U}^k, \mathbf{V}^{k-1}, \hat{b}^k), b - \hat{b}^k \rangle + \frac{L_v^k}{2} (b - \hat{b}^k)^2, \quad (13)$$

where L_u^k and L_v^k are stepsize parameters, which will be discussed later. One of the benefits of using proximal descent is that it results in closed-form solutions.

Theorem 1. *Subproblems (10), (11), (12) and (13) have the following closed-form solutions:*

$$\mathbf{U}^k = \mathcal{S}_{\tau_u} \left(\mathbf{U}^{k-1} - \frac{1}{L_u^k} \nabla_{\mathbf{U}} \mathcal{L}(\mathbf{U}^{k-1}, \mathbf{V}^{k-1}, b^{k-1}) \right), \quad (14)$$

$$\hat{b}^k = b^{k-1} - \frac{1}{L_u^k} \nabla_b \mathcal{L}(\mathbf{U}^{k-1}, \mathbf{V}^{k-1}, b^{k-1}), \quad (15)$$

$$\mathbf{V}^k = \mathcal{S}_{\tau_v} \left(\mathbf{V}^{k-1} - \frac{1}{L_v^k} \nabla_{\mathbf{V}} \mathcal{L}(\mathbf{U}^k, \mathbf{V}^{k-1}, \hat{b}^k) \right), \quad (16)$$

$$b^k = \hat{b}^k - \frac{1}{L_v^k} \nabla_b \mathcal{L}(\mathbf{U}^k, \mathbf{V}^{k-1}, \hat{b}^k), \quad (17)$$

where $\tau_u = \lambda/(L_u^k \cdot \|\hat{\mathbf{u}}_j\|_2)$, $\tau_v = \lambda/(L_v^k \cdot \|\hat{\mathbf{v}}_k\|_2)$, $\mathcal{S}_{\tau_u}(\cdot)$ and $\mathcal{S}_{\tau_v}(\cdot)$ are respectively the row-wise and column-wise soft-thresholding operator, which are defined below:

$$(\mathcal{S}_{\tau_u}(\mathbf{u}))_j = \begin{cases} \mathbf{u}_j - \tau_u \gamma \frac{\mathbf{u}_j}{\|\mathbf{u}_j\|_2}, & \text{if } \|\mathbf{u}_j\|_2 > \tau_u \gamma \\ \mathbf{0}, & \text{if } \|\mathbf{u}_j\|_2 \leq \tau_u \gamma \end{cases} \quad (18)$$

$$(\mathcal{S}_{\tau_v}(\mathbf{v}))_k = \begin{cases} \mathbf{v}_k - \tau_v \gamma \frac{\mathbf{v}_k}{\|\mathbf{v}_k\|_2}, & \text{if } \|\mathbf{v}_k\|_2 > \tau_v \gamma \\ \mathbf{0}, & \text{if } \|\mathbf{v}_k\|_2 \leq \tau_v \gamma \end{cases} \quad (19)$$

for $j = 1, 2, \dots, s$ and $k = 1, 2, \dots, t$, where $\gamma = \sqrt{r}$. Here, r is the length of \mathbf{u}_j and \mathbf{v}_k (they have the same length).

The proof of Theorem 1 can be found in the Appendix. We summarize the proposed BCPD algorithm in the table below.

Algorithm Block Coordinate Proximal Descent

Input: $\{\mathbf{X}_i, y_i\}_{i=1}^n$

Initialization: Randomly choose $(\mathbf{U}^0, \mathbf{V}^0, b^0)$

while convergence criterion not met **do**

 Compute $(\mathbf{U}^k, \hat{b}^k)$ using (14) and (15)

 Compute (\mathbf{V}^k, b^k) using (16) and (17)

 Let $k = k + 1$

end while

To guarantee fast convergence, the stepsize parameters L_u^k and L_v^k are usually obtained from Lipschitz constants, which satisfy the following inequalities:

$$\|\nabla_{(\mathbf{U}, b)} \mathcal{L}(\mathbf{U}, \mathbf{V}^{k-1}, b) - \nabla_{(\mathbf{U}, b)} \mathcal{L}(\tilde{\mathbf{U}}, \mathbf{V}^{k-1}, \tilde{b})\|_F \leq L_u^k \|\mathbf{U}, b) - (\tilde{\mathbf{U}}, \tilde{b})\|_F, \quad (20)$$

$$\|\nabla_{(\mathbf{V}, b)} \mathcal{L}(\mathbf{U}^k, \mathbf{V}, b) - \nabla_{(\mathbf{V}, b)} \mathcal{L}(\mathbf{U}^k, \tilde{\mathbf{V}}, \tilde{b})\|_F \leq L_v^k \|\mathbf{V}, b) - (\tilde{\mathbf{V}}, \tilde{b})\|_F, \quad (21)$$

where $\|(\mathbf{U}, b)\|_F = \sqrt{\|\mathbf{U}\|_F^2 + b^2}$ and $\|(\mathbf{V}, b)\|_F = \sqrt{\|\mathbf{V}\|_F^2 + b^2}$. For some of the distributions in the exponential family, we can easily derive the Lipschitz constants of their derivative function. For example, we have the following Lipschitz constants if the response variable of the generalized matrix regression is from a normal distribution or a logistic distribution (detailed derivation can be found in the Appendix):

$$L_u = \sqrt{2} \sum_{i=1}^n \left(1 + \|\mathbf{X}_i \mathbf{V}^\top\|_F\right) \|1 + \mathbf{X}_i \mathbf{V}^\top\|_F, \quad (22)$$

$$L_v = \sqrt{2} \sum_{i=1}^n \left(1 + \|\mathbf{U}^\top \mathbf{X}_i\|_F\right) \|1 + \mathbf{U}^\top \mathbf{X}_i\|_F. \quad (23)$$

The convergence criterion for the BCPD algorithm is defined using the relative objective function improvement and the relative change of the coefficient matrix:

$$q^k \equiv \max \left\{ \frac{\|\mathbf{B}^k - \mathbf{B}^{k-1}\|_F}{1 + \|\mathbf{B}^{k-1}\|_F}, \frac{|F^k - F^{k-1}|}{1 + F^{k-1}} \right\} \leq \epsilon, \quad (24)$$

where ϵ is a small number (e.g., 10^{-4}), $F^k = \mathcal{L}(\mathbf{U}^k, \mathbf{V}^k, b^k) + \mathcal{R}(\mathbf{U}^k, \mathbf{V}^k)$ is the objective function, and $\mathbf{B}^k = \mathbf{U}^k \mathbf{V}^k$ is the coefficient matrix.

Theorem 2 indicates that the BCPD algorithm has a global convergence property, which implies that it converges to a critical point of optimization criterion (6) with any initialization.

Theorem 2. *The sequence generated by the proposed BCPD algorithm converges to a critical point of the optimization criterion (6).*

The proof for Theorem 2 can be found in the Appendix.

4 Simulation Study

4.1 Data Generation

In this section, we validate the performance of our 2D variable selection method using simulated datasets. Specifically, we randomly generate two factor matrices $\mathbf{U} \in \mathbb{R}^{s \times r}$ and $\mathbf{V} \in \mathbb{R}^{r \times t}$ using MATLAB command `rand(s, r) * 2 - 1` and `rand(r, t) * 2 - 1`, where $s = 10, t = 10, r = 3$. We then let the 1st, 3rd, 5th, 7th, 9th row of \mathbf{U} and the 2nd, 4th, 6th, 8th, 10th column of \mathbf{V} be zeros. The coefficient matrix is generated using $\mathbf{B} = \mathbf{U}\mathbf{V}$. All dataset is generated from the same random seed using MATLAB command `rng('default')`.

We consider three scenarios for the generation of process variable matrix \mathbf{X}_i : (i) IID, (ii) row correlated, and (iii) spatio-temporal correlated. In the first scenario, all the entries of \mathbf{X}_i are generated from a IID standard normal distribution. In the second scenario, we let the correlation between the row j and row k of matrix \mathbf{X}_i be $0.5^{|j-k|}$ to mimic the correlation among process variables. In the third scenario, we let the spatio-temporal correlation between each of the row j and column k of matrix \mathbf{X}_i be $0.5^{|j-k|}$ setting a spatial scale parameter $\phi_s = 0.3$ and a spatial variance $\sigma_s^2 = 1$. For all scenario, an IID noise matrix \mathbf{E}_i , each entry of which is from a standard normal distribution $\mathcal{N}(0, \sigma^2)$, is added to \mathbf{X}_i . Here, σ is determined using a signal-noise-ratio (SNR), which is defined as $SNR = n\sigma / \sum_{i=1}^n \|\mathbf{X}_i\|_F$. We consider three levels of SNR, i.e., $\alpha = 0, 0.5, 1.0$ for (i) IID and (ii) row correlated scenarios and $\alpha = 0, 0.5, 0.8$ for (iii) spatio-temporal correlated scenario, which are denoted by “no noise”, “low noise”, and “high noise”, respectively. In addition, we generated datasets with different sample size $n = 100, 200, 500$. The product quality index is generated using a logistic regression model $\log(\frac{y_i}{1-y_i}) = b + \langle \mathbf{B}, \mathbf{X}_i + \mathbf{E}_i \rangle$, where $b = 0$. The generated data $\{\mathbf{X}_i, y_i\}_{i=1}^n$ are then used to validate the performance of our model. The stopping criteria is set as $q^k < 10^{-4}$ and the maximum number of iteration is 1500.

The performance of our model is compared to two benchmarks. The first benchmark, designated as “Row-Column,” first applies adaptive group LASSO to select the crucial rows of the process variable matrix \mathbf{X}_i . Then, the identified non-crucial rows are removed from \mathbf{X}_i , and adaptive group LASSO is applied again to select the crucial columns. The second benchmarking model, which we refer to as “Column-Row,” is similar to the first benchmark except that it selects the crucial columns first and then identifies the crucial rows.

Since the optimization problem for our 2D variable selection method is nonconvex, the initial point is important for both the solution quality and convergence speed. Therefore, we propose the following heuristic method for parameter initialization. Specifically, we first regress each element of \mathbf{X}_i against y_i , and combine the estimated coefficient from all the elements to construct a matrix $\tilde{\mathbf{B}}$. Next, we apply singular value decomposition (SVD) on $\tilde{\mathbf{B}}$, and set \mathbf{U}^0 to the first r (rank) left singular vectors and \mathbf{V}^0 to the first r right singular vectors of $\tilde{\mathbf{B}}$. Various ranks are tested and the best rank is selected using AIC.

4.2 Results and Analysis

We apply our 2D variable selection method as well as the two benchmarks to the generated datasets. We compute the selection accuracy using the following equation:

$$\text{Accuracy} = \frac{\text{TP} + \text{TN}}{\text{Number of rows} + \text{Number of columns}}, \quad (25)$$

where ‘‘TP’’ represents ‘‘True Positive’’, which is the number of crucial rows and columns that are selected correctly. ‘‘TN’’ represents ‘‘True Negative’’, which is the number of non-crucial rows and columns that are removed correctly.

We repeat the whole simulation process for 100 times and report the mean selection accuracies and corresponding standard deviations (SD) in Tables 2, 3, and 4 below.

Noise Level (SNR)	Method	Sample Size	True Positive	True Negative	False Positive	False Negative	Accuracy (SD)
No Noise ($\alpha = 0$)	Proposed Method	100	99.2	94.1	0.8	5.9	96.7 (6.44)
		200	99.2	99.4	0.8	0.6	99.3 (1.88)
		500	100.0	100.0	0.0	0.0	100.0 (0.00)
	Benchmark I	100	95.7	90.1	4.3	9.9	92.9 (6.44)
		200	98.6	99.5	1.4	0.5	99.1 (2.90)
		500	100.0	100.0	0.0	0.0	100.0 (0.00)
	Benchmark II	100	97.8	88.7	2.2	11.3	93.3 (4.46)
		200	98.7	97.8	1.3	2.2	98.3 (2.40)
		500	99.9	100.0	0.1	0.0	100.0 (0.50)
Low Noise ($\alpha = 0.5$)	Proposed Method	100	98.2	93.4	1.8	6.6	95.8 (3.23)
		200	98.8	99.4	1.2	0.6	99.1 (2.29)
		500	100.0	100.0	0.0	0.0	100.0 (0.00)
	Benchmark I	100	93.7	89.5	6.3	10.5	91.6 (6.85)
		200	98.2	99.6	1.8	0.4	98.9 (3.06)
		500	100.0	100.0	0.0	0.0	100.0 (0.00)
	Benchmark II	100	96.9	88.4	3.1	11.6	92.7 (4.74)
		200	98.1	97.6	1.9	2.4	97.9 (2.59)
		500	99.8	100.0	0.2	0.0	99.9 (0.70)
High Noise ($\alpha = 1.0$)	Proposed Method	100	96.3	93.2	3.7	6.8	94.8 (3.72)
		200	98.3	99.2	1.7	0.8	98.8 (2.79)
		500	99.6	100.0	0.4	0.0	99.8 (0.98)
	Benchmark I	100	89.0	89.5	11.0	10.5	89.3 (7.50)
		200	96.5	99.5	3.5	0.5	98.0 (4.14)
		500	98.1	100.0	1.9	0.0	99.1 (4.42)
	Benchmark II	100	92.1	89.3	7.9	10.7	90.7 (8.04)
		200	96.0	98.2	4.0	1.8	97.1 (3.71)
		500	96.3	100.0	3.7	0.0	98.2 (4.59)

Table 2: Average true positive (%), true negative (%), false positive (%), false negative (%), selection accuracy (%) for \mathbf{X}_i with IID entries.

Noise Level (SNR)	Method	Sample Size	True Positive	True Negative	False Positive	False Negative	Accuracy (SD)
No Noise ($\alpha = 0$)	Proposed Method	100	97.2	93.4	2.8	6.6	95.3 (3.75)
		200	99.4	99.5	0.6	0.5	99.5 (1.57)
		500	100.0	100.0	0.0	0.0	100.0 (0.0)
	Benchmark I	100	89.1	84.3	10.9	15.7	86.7 (7.11)
		200	85.9	99.0	14.1	1.0	92.5 (7.54)
		500	87.2	100.0	12.8	0.0	93.6 (4.43)
	Benchmark II	100	94.6	87.1	5.4	12.9	90.9 (5.99)
		200	96.6	98.0	3.4	2.0	97.3 (3.79)
		500	99.8	100.0	0.2	0.0	99.9 (1.00)
Low Noise ($\alpha = 0.5$)	Proposed Method	100	96.1	93.3	3.9	6.7	94.7 (4.65)
		200	98.4	99.5	1.6	0.5	99.0 (2.39)
		500	100.0	100.0	0.0	0.0	100.0 (0.00)
	Benchmark I	100	86.7	85.0	13.3	15.0	85.9 (7.95)
		200	85.0	98.7	15.0	1.3	91.9 (7.74)
		500	87.3	100.0	12.7	0.0	93.7 (4.43)
	Benchmark II	100	93.4	87.4	6.6	12.6	90.4 (5.76)
		200	95.8	98.3	4.2	1.7	97.1 (4.98)
		500	99.8	100.0	0.2	0.0	99.9 (0.70)
High Noise ($\alpha = 1.0$)	Proposed Method	100	92.0	92.3	8.0	7.7	92.2 (6.83)
		200	97.2	99.2	2.8	0.8	98.2 (3.37)
		500	99.3	100.0	0.7	0.0	99.7 (1.28)
	Benchmark I	100	78.5	87.4	21.5	12.6	83.0 (10.66)
		200	82.2	99.5	17.8	0.5	90.9 (8.50)
		500	86.9	100.0	13.1	0.0	93.5 (5.11)
	Benchmark II	100	87.4	89.7	12.6	10.3	88.6 (7.73)
		200	91.0	99.0	9.0	1.0	95.0 (7.07)
		500	97.9	100.0	2.1	0.0	99.0 (3.12)

Table 3: Average true positive (%), true negative (%), false positive (%), false negative (%), selection accuracy (%) for \mathbf{X}_i with row correlated entries.

Tables 2, 3, and 4 indicate that our proposed 2D variable selection method always achieves higher selection accuracy than the two benchmarks under all scenarios (i.e., noise level, sample size, and correlation pattern). For example, for \mathbf{X}_i with IID entries, without noise, and small sample size ($n = 100$), the average selection accuracy for our 2D variable selection method is 96.7%, whereas they are 92.9% and 93.3% for benchmarks I and II, respectively. For \mathbf{X}_i with row correlated entries, with low noise, and medium sample size ($n = 200$), the selection accuracy for our 2D variable selection method and the two benchmarking models are 99.0%, 91.9%, and 97.1%, respectively. Note that we set row j and row k of matrix \mathbf{X}_i correlated in this scenario. Thus, benchmark II (column-row selection) is better than benchmark I (row-column selection) in terms of selection accuracy, because columns are still IID. Despite of this observation, our proposed method is always better than two benchmarks. Another example, for \mathbf{X}_i with spatio-temporal correlated entries, with high noise, and large sample size ($n = 500$), the accuracy for our 2D variable selection

Noise Level (SNR)	Method	Sample Size	True Positive	True Negative	False Positive	False Negative	Accuracy (SD)
No Noise ($\alpha = 0$)	Proposed Method	100	95.6	85.7	4.4	14.3	90.7 (5.25)
		200	86.0	95.9	14.0	4.1	91.0 (7.34)
		500	89.3	99.8	10.7	0.2	94.6 (6.44)
	Benchmark I	100	79.2	79.4	20.8	20.6	79.3 (8.59)
		200	71.3	93.0	28.7	7.0	82.2 (8.51)
		500	60.0	100.0	40.0	0.0	80.0 (6.59)
	Benchmark II	100	76.9	81.9	23.1	18.1	79.4 (7.99)
		200	71.1	94.7	28.9	5.3	82.9 (8.77)
		500	65.6	100.0	34.4	0.0	82.8 (6.49)
Low Noise ($\alpha = 0.5$)	Proposed Method	100	93.6	84.4	6.4	15.6	89.0 (6.03)
		200	87.0	95.5	13.0	4.5	91.3 (6.17)
		500	89.4	99.7	10.6	0.3	94.6 (6.75)
	Benchmark I	100	76.0	80.0	24.0	20.0	78.0 (9.48)
		200	67.3	95.0	32.7	5.0	81.2 (9.40)
		500	60.5	100.0	39.5	0.0	80.3 (6.94)
	Benchmark II	100	76.1	81.4	23.9	18.6	78.8 (8.94)
		200	70.7	96.0	29.3	4.0	83.4 (8.96)
		500	66.7	100.0	33.3	0.0	83.4 (7.00)
High Noise ($\alpha = 0.8$)	Proposed Method	100	91.0	84.5	9.0	15.5	87.8 (6.79)
		200	84.4	95.7	15.6	4.3	90.1 (6.87)
		500	87.5	99.6	12.5	0.4	93.6 (6.72)
	Benchmark I	100	73.5	80.9	26.5	19.1	77.2 (9.62)
		200	62.9	96.3	37.1	3.7	79.6 (9.68)
		500	61.9	100.0	38.1	0.0	81.0 (6.73)
	Benchmark II	100	73.0	82.5	27.0	17.5	77.8 (9.81)
		200	66.5	97.2	33.5	2.8	81.9 (10.60)
		500	67.6	100.0	32.4	0.0	83.8 (6.89)

Table 4: Average true positive (%), true negative (%), false positive (%), false negative (%), selection accuracy (%) for \mathbf{X}_i with spatio-temporal correlated entries.

method and the two benchmarks are 93.6%, 81.0%, and 83.8%, respectively. We believe the reason why our proposed method performs better than the two benchmarks is that our method simultaneously selects the crucial rows and columns, whereas the benchmarks identifies the rows (or columns) first then columns (or rows) sequentially. Sequential selection compromises the selection accuracy since when identifying the crucial rows, the elements from the columns that are not crucial negatively affect the selection result, vice versa.

5 Case Study

In this section, we apply our proposed 2D variable selection method to a real-world dataset. The dataset is from the hot strip mill illustrated in Figure 1. The primary function of the hot strip mill is to reheat semi-

finished steel slabs nearly to their melting point, then roll them thinner and longer through 7 successive rolling mill stands driven by motors, and finally coiling up the lengthened steel sheet for transport to the next process.

The dataset consists of 490 strip steel products made using the same hot strip mill. Among the 490 samples, 264 of them are good quality products and the remaining 226 are products with bad quality. The product quality is defined based on the percentage of width defects. Specifically, the width of each steel strip was measured at 1500 locations uniformly distributed along the strip. Any measurement point whose width is smaller than a predefined width threshold is considered as a defect point. The quality index is then computed by dividing the number of defects over 1500. Therefore, the range of the quality index is $[0, 1]$. Each sample has 9 process variables: target speed of rollers, measured speed of rollers, looper value (used to control the tension of a steel strip), target force on both side of the rollers, measured force on the work side of rollers, measured force on the transfer side of rollers, roller gap, looper height (also used to control the tension of a steel strip), and temperature. At each stage, each of the process variable is a profile with 1500 points observed during the steel strip rolling process. We take the average of each profile and set it as the value of that process variable. As a result, for each sample, we construct a process variable matrix X_i with 9 rows and 7 columns.

To get a stable selection result, we randomly select 400 samples from the dataset and construct a sub dataset. We then apply our proposed method to the sub dataset to identify crucial rows and columns. We repeat this procedure for 100 times and then compute the selection percentage for each row and column of the process variable matrix. Any row (or column) whose selection rate is higher than 0.5 is considered as an important row (or column).

As a result, the identified crucial process variables are temperature, looper value and looper height; the identified crucial stages are stage 5, 6 and 7. After discussing with the engineers in the steel company who provides us the data, we conclude that the selection results are reasonable. To be specific, temperature is one of the most important and sensitive control variables for a hot strip mill. A slight change in temperature may result in a significant change in product quality. In addition, looper value and looper height are two highly correlated variables. Selecting both of them implies that there is something wrong with the looper control for stages 5, 6, and 7. This is confirmed by the fact that stages 1-4 of the hot roll mill respectively has a reducer connected to the rollers to reduce the speed from the driven motors, whereas stages 5-7 do not have any reducer. Therefore, the feedback control for the looper at stages 5-7 are more challenging.

6 Conclusions

The advancements in sensing technology and data acquisition systems have facilitated us to collect massive amount of control and sensor data during the operation of multistage processes. These kind of data is often generated in the form of a matrix. The matrix-formed data contain rich information containing a large amount of control and sensor data with multistage process and can be utilized for diagnostics for product quality defects. Conventionally, LASSO [4] have been used to identify any process variable with a nonzero coefficient considered to be responsible for quality defects. However, one the limitations of LASSO is that it cannot deal with structured data. For structured data, group LASSO [9] is widely used to identify crucial process variables and stages regrading rows (column) as process variables (stages) to be selected first and columns (row) as stages (process variables) to be selected second sequentially. However, the column (row) selection is negatively affected by the non-crucial rows (columns). Thus, it is important to consider rows and columns at the same time so that each group selection does not affect the other group selection. However, the analysis of structured data become challenging due to complex correlation between the entries of them.

In this paper, we proposed a 2D variable selection methodology. The method regresses a matrix-based

independent variable against a response variable using a generalized linear model to extend when a response variable is any exponential family distribution. To simultaneously identify the crucial rows and columns of the matrix, we decompose the unknown regression coefficient matrix as a produce of two factor matrices, and penalize the rows of the first factor matrix and columns of the second matrix using adaptive group LASSO. To estimate the penalized factor matrices, we developed a block coordinate proximal descent optimization algorithm. The algorithm transfers the optimization problem into two sub optimization problems by iteratively optimizing one factor matrix while keeping the other one fixed. We proved that the subproblems have closed-form solutions, which help significantly speed up the computation process. In addition, we proved that the proposed block coordinate proximal descent algorithm can always converge to a critical point of the optimization problem.

A simulation study was carried out to evaluate the performance of the proposed method. The results indicated our proposed method always achieves higher selection accuracy than the two benchmarks under all scenarios (i.e., noise level, sample size, and correlation pattern). For example, the mean accuracy for \mathbf{X}_i with spatio-temporal correlated entries, with high noise, and large sample size ($n = 500$), the accuracy for our 2D variable selection method and the two benchmarks are 93.6%, 81.0%, and 83.8%, respectively. We believe this is because our method simultaneously selects the crucial rows and columns of a matrix, and thus can reduce the negative effect from the non-crucial entries. We also validate the effectiveness of our method using a case study on real-world quality defect diagnostics application in steel industry. As an example, we indentify temperature, looper value and looper height as the crucial process variables and stage 5, 6 and 7 as the crucial stages. This is reasonable since the process variables and stages are logically explainable for the quality defects in the process of manufacturing a desired still sheet for the next use. Even though our method developed in this paper has closed form solutions, the convergence speed of a penalized matrix regression need to be more accelerated. This is an important topic for future research.

Appendices

A Proof for Theorem 1

Equations (15) and (17) can be easily proved using gradient descent. Therefore, we only prove Equations (14) and (16) here. The regularization term $\mathcal{R}(\mathbf{U}, \mathbf{V})$ in Equation (7) can be decomposed as $\mathcal{R}(\mathbf{U}, \mathbf{V}) = \mathcal{R}_1(\mathbf{U}) + \mathcal{R}_2(\mathbf{V})$, where

$$\mathcal{R}_1(\mathbf{U}) = \lambda\gamma \sum_{j=1}^s \frac{\|\mathbf{u}_j\|_2}{\|\hat{\mathbf{u}}_j\|_2},$$

$$\mathcal{R}_2(\mathbf{V}) = \lambda\gamma \sum_{k=1}^t \frac{\|\mathbf{v}_k\|_2}{\|\hat{\mathbf{v}}_k\|_2}.$$

Here, $\lambda \geq 0$ is the tuning parameter. $\|\cdot\|_2$ is ℓ_2 norm. $\gamma = \sqrt{r}$. $\mathbf{u}_j \in \mathbb{R}^r$ is the j th row of matrix \mathbf{U} and $\mathbf{v}_k \in \mathbb{R}^r$ is the k th column of matrix \mathbf{V} . $\hat{\mathbf{u}}_j$ and $\hat{\mathbf{v}}_k$ are the maximum likelihood estimates of \mathbf{u}_j and \mathbf{v}_k when $\lambda = 0$, respectively.

To derive the closed-form solutions for Equations (10) and (12), we first introduce Moreau decomposition. To be specific, let $\text{prox}(\cdot)$ be the proximal operator and \mathcal{R}_1^* be the conjugate of \mathcal{R}_1 . Moreau decomposition for the term \mathcal{R}_1 is as follows:

$$\mathbf{U} = \text{prox}_{\mathcal{R}_1}(\mathbf{U}) + \text{prox}_{\mathcal{R}_1^*}(\mathbf{U}).$$

where

$$\begin{aligned}\mathbf{U} &= (\mathbf{u}_1, \mathbf{u}_2, \dots, \mathbf{u}_s), \\ \text{prox}_{\mathcal{R}_1}(\mathbf{U}) &= (\text{prox}_{\mathcal{R}_{11}}(\mathbf{u}_1), \text{prox}_{\mathcal{R}_{12}}(\mathbf{u}_2), \dots, \text{prox}_{\mathcal{R}_{1s}}(\mathbf{u}_s)), \\ \text{prox}_{\mathcal{R}_1^*}(\mathbf{U}) &= (\text{prox}_{\mathcal{R}_{11}^*}(\mathbf{u}_1), \text{prox}_{\mathcal{R}_{12}^*}(\mathbf{u}_2), \dots, \text{prox}_{\mathcal{R}_{1s}^*}(\mathbf{u}_s)).\end{aligned}$$

Note that Moreau decomposition is a generalization of the classical orthogonal decomposition, so we can represent the proximal operator of the conjugate as a projection operator $\mathcal{P}(\cdot)$:

$$\text{prox}_{\mathcal{R}_{1j}}(\mathbf{u}_j) = \mathbf{u}_j - \mathcal{P}_{\mathcal{B}_*(\tau_u\gamma)}(\mathbf{u}_j),$$

where

$$\begin{aligned}\mathcal{R}_{1j} &= \lambda\gamma \frac{\|\mathbf{u}_j\|_2}{\|\hat{\mathbf{u}}_j\|_2}, \quad \forall j = 1, 2, \dots, s \quad \text{and} \\ \mathcal{B}_*(\tau_u\gamma) &= \left\{ \mathbf{u}_j \in \mathbb{R}^r : \|\mathbf{u}_j\|_2 \leq \tau_u\gamma, \text{ where } \tau_u = \frac{\lambda}{L_u^k \|\hat{\mathbf{u}}_j\|_2}, \gamma = \sqrt{r}, \forall j = 1, 2, \dots, s \right\}\end{aligned}$$

is the ball of dual norm. Therefore, the proximal operator of the conjugate of the term \mathcal{R}_1 becomes a projection onto the ball of the dual norm, which is expressed by:

$$\mathcal{P}_{\mathcal{B}_*(\tau_u\gamma)}(\mathbf{u}_j) = \begin{cases} \tau_u\gamma \frac{\mathbf{u}_j}{\|\mathbf{u}_j\|_2}, & \text{if } \|\mathbf{u}_j\|_2 > \tau_u\gamma \\ \mathbf{u}_j, & \text{if } \|\mathbf{u}_j\|_2 \leq \tau_u\gamma \end{cases}$$

Therefore, we can derive a closed-form solution for BCPD, which is the row-wise soft-thresholding operator $(\mathcal{S}_{\tau_u})_j$ shown below:

$$(\mathcal{S}_{\tau_u}(\mathbf{u}))_j = \text{prox}_{\mathcal{R}_1}(\mathbf{u}_j) = \begin{cases} \mathbf{u}_j - \tau_u\gamma \frac{\mathbf{u}_j}{\|\mathbf{u}_j\|_2}, & \text{if } \|\mathbf{u}_j\|_2 > \tau_u\gamma \\ \mathbf{0}, & \text{if } \|\mathbf{u}_j\|_2 \leq \tau_u\gamma \end{cases}$$

The column-wise soft-thresholding operator $(\mathcal{S}_{\tau_v})_k$ can be derived similarly. \square

B Derivations of the Lipschitz constants

For a Binomial distribution, we have the following:

$$\begin{aligned}\mathbb{P}(y|\mathbf{X}; \mathbf{B}, b) &= \exp \left\{ y_i (b + \langle \mathbf{X}_i \mathbf{V}^\top, \mathbf{U} \rangle) - \log (1 + \exp [b + \langle \mathbf{X}_i \mathbf{V}^\top, \mathbf{U} \rangle]) \right\}, \\ \mathcal{L}(\mathbf{U}, \mathbf{V}, b) &= - \sum_{i=1}^n \left\{ y_i (b + \langle \mathbf{X}_i \mathbf{V}^\top, \mathbf{U} \rangle) - \log (1 + \exp [b + \langle \mathbf{X}_i \mathbf{V}^\top, \mathbf{U} \rangle]) \right\}, \\ \nabla_{(\mathbf{U}, b)} \mathcal{L}(\mathbf{U}, \mathbf{V}, b) &= \nabla_{(\mathbf{U}, b)} \left\{ - \sum_{i=1}^n \left(y_i (b + \langle \mathbf{X}_i \mathbf{V}^\top, \mathbf{U} \rangle) - \log (1 + \exp [b + \langle \mathbf{X}_i \mathbf{V}^\top, \mathbf{U} \rangle]) \right) \right\} \\ &= - \sum_{i=1}^n \left(y_i - (1 + \exp [-b - \langle \mathbf{X}_i \mathbf{V}^\top, \mathbf{U} \rangle])^{-1} \right) (1 + \mathbf{X}_i \mathbf{V}^\top).\end{aligned}$$

$$\begin{aligned}
& \|\nabla_{(\mathbf{U}, b)} \mathcal{L}(\mathbf{U}, \mathbf{V}, b) - \nabla_{(\mathbf{U}, b)} \mathcal{L}(\tilde{\mathbf{U}}, \mathbf{V}, \tilde{b})\|_F \\
& \leq \left\| -\sum_{i=1}^n \left\{ (1 + \exp[-b - \langle \mathbf{X}_i \mathbf{V}^\top, \mathbf{U} \rangle])^{-1} - (1 + \exp[-\tilde{b} - \langle \mathbf{X}_i \mathbf{V}^\top, \tilde{\mathbf{U}} \rangle])^{-1} \right\} (1 + \mathbf{X}_i \mathbf{V}^\top) \right\|_F \\
& \leq \sum_{i=1}^n \left| (1 + \exp[-b - \langle \mathbf{X}_i \mathbf{V}^\top, \mathbf{U} \rangle])^{-1} - (1 + \exp[-\tilde{b} - \langle \mathbf{X}_i \mathbf{V}^\top, \tilde{\mathbf{U}} \rangle])^{-1} \right| \|1 + \mathbf{X}_i \mathbf{V}^\top\|_F \\
& \leq \sum_{i=1}^n \left| -b - \langle \mathbf{X}_i \mathbf{V}^\top, \mathbf{U} \rangle + \tilde{b} - \langle \mathbf{X}_i \mathbf{V}^\top, \tilde{\mathbf{U}} \rangle \right| \|1 + \mathbf{X}_i \mathbf{V}^\top\|_F \\
& \leq \sum_{i=1}^n \left(\left| \langle \mathbf{X}_i \mathbf{V}^\top, \mathbf{U} - \tilde{\mathbf{U}} \rangle \right| + |b - \tilde{b}| \right) \|1 + \mathbf{X}_i \mathbf{V}^\top\|_F \\
& \leq \sum_{i=1}^n \left(\|\mathbf{X}_i \mathbf{V}^\top\|_F \|\mathbf{U} - \tilde{\mathbf{U}}\|_F + |b - \tilde{b}| \right) \|1 + \mathbf{X}_i \mathbf{V}^\top\|_F \\
& \leq \sum_{i=1}^n \left(\|\mathbf{U} - \tilde{\mathbf{U}}\|_F + |b - \tilde{b}| \right) \left(1 + \|\mathbf{X}_i \mathbf{V}^\top\|_F \right) \|1 + \mathbf{X}_i \mathbf{V}^\top\|_F \\
& \leq \sqrt{2} \sum_{i=1}^n \left(1 + \|\mathbf{X}_i \mathbf{V}^\top\|_F \right) \|1 + \mathbf{X}_i \mathbf{V}^\top\|_F \|(\mathbf{U}, b) - (\tilde{\mathbf{U}}, \tilde{b})\|_F.
\end{aligned}$$

where in the third inequality we used the fact that

$$|(1 + e^x)^{-1} - (1 + e^y)^{-1}| \leq |x - y|,$$

and in the seventh inequality we used the Cauchy-Schwarz inequality

$$\|\mathbf{U} - \tilde{\mathbf{U}}\|_F + |b - \tilde{b}| \leq \sqrt{2} \|(\mathbf{U}, b) - (\tilde{\mathbf{U}}, \tilde{b})\|_F.$$

The constant L_v can be derived similarly. \square

For a normal distribution, we have the following:

$$\begin{aligned}
\mathbb{P}(y|\mathbf{X}; \mathbf{B}, b) &= \exp \left\{ y_i (b + \langle \mathbf{X}_i \mathbf{V}^\top, \mathbf{U} \rangle) + \frac{1}{2} \|b + \langle \mathbf{X}_i \mathbf{V}^\top, \mathbf{U} \rangle\|^2 \right\}, \\
\mathcal{L}(\mathbf{U}, \mathbf{V}, b) &= -\sum_{i=1}^n \left\{ (y_i (b + \langle \mathbf{X}_i \mathbf{V}^\top, \mathbf{U} \rangle) + \frac{1}{2} \|b + \langle \mathbf{X}_i \mathbf{V}^\top, \mathbf{U} \rangle\|^2) \right\}, \\
\nabla_{(\mathbf{U}, b)} \mathcal{L}(\mathbf{U}, \mathbf{V}, b) &= \nabla_{(\mathbf{U}, b)} \left\{ -\sum_{i=1}^n \left(y_i (b + \langle \mathbf{X}_i \mathbf{V}^\top, \mathbf{U} \rangle) + \frac{1}{2} \|b + \langle \mathbf{X}_i \mathbf{V}^\top, \mathbf{U} \rangle\|^2 \right) \right\} \\
&= -\sum_{i=1}^n \left(y_i - b - \langle \mathbf{X}_i \mathbf{V}^\top, \mathbf{U} \rangle \right) (1 + \mathbf{X}_i \mathbf{V}^\top).
\end{aligned}$$

$$\begin{aligned}
& \|\nabla_{(\mathbf{U}, b)} \mathcal{L}(\mathbf{U}, \mathbf{V}, b) - \nabla_{(\mathbf{U}, b)} \mathcal{L}(\tilde{\mathbf{U}}, \mathbf{V}, \tilde{b})\|_F \\
& \leq \left\| -\sum_{i=1}^n (y_i - b + \langle \mathbf{X}_i \mathbf{V}^\top, \mathbf{U} \rangle - y_i - \tilde{b} + \langle \mathbf{X}_i \mathbf{V}^\top, \tilde{\mathbf{U}} \rangle) (1 + \mathbf{X}_i \mathbf{V}^\top) \right\|_F \\
& \leq \sum_{i=1}^n \left| -b - \langle \mathbf{X}_i \mathbf{V}^\top, \mathbf{U} \rangle + \tilde{b} + \langle \mathbf{X}_i \mathbf{V}^\top, \tilde{\mathbf{U}} \rangle \right| \|1 + \mathbf{X}_i \mathbf{V}^\top\|_F \\
& \leq \sum_{i=1}^n \left(\left| \langle \mathbf{X}_i \mathbf{V}^\top, \mathbf{U} - \tilde{\mathbf{U}} \rangle \right| + |b - \tilde{b}| \right) \|1 + \mathbf{X}_i \mathbf{V}^\top\|_F \\
& \leq \sum_{i=1}^n \left(\|\mathbf{X}_i \mathbf{V}^\top\|_F \|\mathbf{U} - \tilde{\mathbf{U}}\|_F + |b - \tilde{b}| \right) \|1 + \mathbf{X}_i \mathbf{V}^\top\|_F \\
& \leq \sum_{i=1}^n \left(\|\mathbf{U} - \tilde{\mathbf{U}}\|_F + |b - \tilde{b}| \right) \left(1 + \|\mathbf{X}_i \mathbf{V}^\top\|_F \right) \|1 + \mathbf{X}_i \mathbf{V}^\top\|_F \\
& \leq \sqrt{2} \sum_{i=1}^n \left(1 + \|\mathbf{X}_i \mathbf{V}^\top\|_F \right) \|1 + \mathbf{X}_i \mathbf{V}^\top\|_F \|\mathbf{U}, b) - (\tilde{\mathbf{U}}, \tilde{b})\|_F.
\end{aligned}$$

where in the second inequality we used the same fact as the one used in the binomial distribution case. \square

C Algorithms for non-Lipschitzness case

Among exponential family distributions, several distributions such as Poisson and Gamma distributions does not have a global upper bound since log-likelihood functions in case of Poisson and Gamma distributions are constructed using an exponential and a logarithmic term [5]. Therefore, they are not globally Lipschitz continous. We can solve problems (10) - (13) using backtracking line search method or deriving local upper bound. However, deriving local upper bound is customized and data dependent approximation of Lipschitz constants. Thus, we introduce a backtracking line search method applied to an accelerated proximal gradient method (Nesterov acceleration) to ensure generally solve the non-Lipschitzness problems. Here are our subproblems to apply the algorithm.

$$\begin{aligned}
\mathbf{U}^k &= \underset{\mathbf{U}}{\operatorname{argmin}} \langle \nabla_{\mathbf{U}} \mathcal{L}(\mathbf{U}^{k-1}, \mathbf{V}^{k-1}, b^{k-1}), \mathbf{U} - \mathbf{U}^{k-1} \rangle + \frac{1}{2t^k} \|\mathbf{U} - \mathbf{U}^{k-1}\|_F^2 + \mathcal{R}_1(\mathbf{U}), \\
\hat{b}^k &= \underset{b}{\operatorname{argmin}} \langle \nabla_b \mathcal{L}(\mathbf{U}^{k-1}, \mathbf{V}^{k-1}, b^{k-1}), b - b^{k-1} \rangle + \frac{1}{2t^k} (b - b^{k-1})^2, \\
\mathbf{V}^k &= \underset{\mathbf{V}}{\operatorname{argmin}} \langle \nabla_{\mathbf{V}} \mathcal{L}(\mathbf{U}^k, \mathbf{V}^{k-1}, \hat{b}^k), \mathbf{V} - \mathbf{V}^{k-1} \rangle + \frac{1}{2s^k} \|\mathbf{V} - \mathbf{V}^{k-1}\|_F^2 + \mathcal{R}_2(\mathbf{V}), \\
b^k &= \underset{b}{\operatorname{argmin}} \langle \nabla_b \mathcal{L}(\mathbf{U}^k, \mathbf{V}^{k-1}, \hat{b}^k), b - \hat{b}^k \rangle + \frac{1}{2s^k} (b - \hat{b}^k)^2,
\end{aligned}$$

where t_k and s_k are stepsize parameters and $\mathcal{R}(\mathbf{U}, \mathbf{V}) = \mathcal{R}_1(\mathbf{U}) + \mathcal{R}_2(\mathbf{V})$.

Algorithm Accelerated Proximal Gradient Method with Backtracking for Regularized GLM

Input: $\{\mathbf{X}_i, y_i\}_{i=1}^n$

Initialization: Take $0 < \alpha < 1$ and $0 < \beta < 1$. Randomly choose $(\mathbf{U}^0, \mathbf{V}^0, b^0) = (\mathbf{U}^{-1}, \mathbf{V}^{-1}, b^{-1})$.

Set $\mathbf{B}^0 = \mathbf{U}^0 \mathbf{V}^0$, $F^0 = \mathcal{L}(\mathbf{U}^0, \mathbf{V}^0, b^0) + \mathcal{R}(\mathbf{U}^0, \mathbf{V}^0)$, $i = 1, j = 1, k = 1, t_1 = 1$, and $s_1 = 1$

while convergence criterion not met **do**

 Set $\tilde{t}_0 = 1$ and $\tilde{s}_0 = 1$

while $\mathcal{L}(\mathbf{U}^i, \mathbf{V}^{k-1}, b^{k-1}) > \mathcal{L}(\tilde{\mathbf{U}}, \mathbf{V}^{k-1}, b^{k-1}) + \langle \nabla_{\mathbf{U}} \mathcal{L}(\tilde{\mathbf{U}}, \mathbf{V}^{k-1}, b^{k-1}), \mathbf{U}^i - \tilde{\mathbf{U}} \rangle + \frac{1}{2\tilde{t}_k} \|\mathbf{U}^i - \tilde{\mathbf{U}}\|_F^2$
 do

 Compute $\tilde{\mathbf{U}} = \mathbf{U}^{i-1} + \frac{i-2}{i+1}(\mathbf{U}^{i-1} - \mathbf{U}^{i-2})$

 Compute $\mathbf{U}^i = \text{prox}_{\mathcal{R}_1 \tilde{t}_i}(\tilde{\mathbf{U}} - \tilde{t}_i \nabla_{\mathbf{U}} \mathcal{L}(\tilde{\mathbf{U}}, \mathbf{V}^{k-1}, b^{k-1}))$

 Set $\tilde{t}_i = \alpha \tilde{t}_{i-1}$

 Set $i = i + 1$

end while

 Update $\mathbf{U}^k = \mathbf{U}^i$

 Set $t_k = \tilde{t}_i$

 Update $\hat{b}^k = b^{k-1} - t_k \nabla_b \mathcal{L}(\mathbf{U}^{k-1}, \mathbf{V}^{k-1}, b^{k-1})$

while $\mathcal{L}(\mathbf{U}^k, \mathbf{V}^j, \hat{b}^k) > \mathcal{L}(\mathbf{U}^k, \tilde{\mathbf{V}}, \hat{b}^k) + \langle \nabla_{\mathbf{V}} \mathcal{L}(\mathbf{U}^k, \tilde{\mathbf{V}}, \hat{b}^k), \mathbf{V}^j - \tilde{\mathbf{V}} \rangle + \frac{1}{2\tilde{s}_k} \|\mathbf{V}^j - \tilde{\mathbf{V}}\|_F^2$ **do**

 Compute $\tilde{\mathbf{V}} = \mathbf{V}^{j-1} + \frac{j-2}{j+1}(\mathbf{V}^{j-1} - \mathbf{V}^{j-2})$

 Compute $\mathbf{V}^j = \text{prox}_{\mathcal{R}_2 \tilde{s}_j}(\tilde{\mathbf{V}} - \tilde{s}_j \nabla_{\mathbf{V}} \mathcal{L}(\mathbf{U}^k, \tilde{\mathbf{V}}, \hat{b}^k))$

 Set $\tilde{s}_j = \beta \tilde{s}_{j-1}$

 Set $j = j + 1$

end while

 Update $\mathbf{V}^k = \mathbf{V}^j$

 Set $s_k = \tilde{s}_j$

 Update $b^k = \hat{b}^k - s_k \nabla_b \mathcal{L}(\mathbf{U}^k, \mathbf{V}^{k-1}, \hat{b}^k)$

 Set $k = k + 1$

end while

where the convergence criterion is as follows:

$$q^k \equiv \max \left\{ \frac{\|\mathbf{B}^k - \mathbf{B}^{k-1}\|_F}{1 + \|\mathbf{B}^{k-1}\|_F}, \frac{|F^k - F^{k-1}|}{1 + F^{k-1}} \right\} \leq \epsilon,$$

Here, we set $F = \mathcal{L}(\mathbf{U}, \mathbf{V}, b) + \mathcal{R}(\mathbf{U}, \mathbf{V})$ as an objective function in (6). The first term $\mathcal{L}(\mathbf{U}, \mathbf{V}, b)$ is convex and differentiable when two of \mathbf{U} , \mathbf{V} , and b fixed. The second term $\mathcal{R}(\mathbf{U}, \mathbf{V}) = \mathcal{R}_1(\mathbf{U}) + \mathcal{R}_2(\mathbf{V})$ is also convex when either \mathbf{U} or \mathbf{V} fixed. The second term is not necessarily differentiable. Therefore, we can use an accelerated (block) proximal gradient method (aka. Nesterov acceleration) with backtracking line search, which ensure to solve non-Lipschitzness problems for regularized GLM, more efficiently than a subgradient or a proximal gradient method. We summarize the algorithm in the table above.

D Proof for Theorem 2

Theorem 2 can be proved following the similar procedures in [8], which establishes global convergence of the cyclic block coordinate proximal method assuming the Kurdyka-Lojasiewicz inequality. Before showing the global convergence property, we introduce the Kurdyka-Lojasiewicz inequality.

Definition. (Kurdyka-Lojasiewicz inequality)

A function $\varphi(\mathbf{x})$ satisfies the Kurdyka-Lojasiewicz inequality (KL) property at point $\bar{\mathbf{x}} \in \text{dom}(\partial\varphi)$ if there exists $\theta \in [0, 1)$ such that

$$\frac{|\varphi(\mathbf{x}) - \varphi(\bar{\mathbf{x}})|^\theta}{\text{dist}(\mathbf{0}, \partial\varphi(\mathbf{x}))}$$

is bounded around $\bar{\mathbf{x}}$. i.e., in a certain neighborhood \mathcal{U} of $\bar{\mathbf{x}}$, there exists $\psi(s) = cs^{1-\theta}$ for some $c > 0$ and $\theta \in [0, 1)$ such that the KL inequality holds

$$\psi'(|\varphi(\mathbf{x}) - \varphi(\bar{\mathbf{x}})|)\text{dist}(\mathbf{0}, \partial\varphi(\mathbf{x})) \geq 1, \text{ for any } \mathbf{x} \in \mathcal{U} \cap \text{dom}(\partial\varphi) \text{ and } \varphi(\mathbf{x}) \neq \varphi(\bar{\mathbf{x}}),$$

where $\text{dom}(\partial\varphi) = \{\mathbf{x} : \partial\varphi \neq \emptyset\}$ and $\text{dist}(\mathbf{0}, \partial\varphi(\mathbf{x})) = \min\{\|\mathbf{y}\| : \mathbf{y} \in \partial\varphi(\mathbf{x})\}$. We can briefly say that, for not only a real analytic function but also a nonsmooth sub-analytic function, the term with $\theta \in [1/2, 1)$ is bounded around any critical point \mathbf{x} , so both a real analytic function and a nonsmooth sub-analytic function satisfies the KL inequality [2, 8].

Note that both real analytic and semi-algebraic functions are sub-analytic. In addition, finite sums of real analytic functions is real analytic, and finite sums of semi-algebraic functions are semi-algebraic. Furthermore, sub-analytic functions map bounded set to bounded set, so the sum of a real analytic function and a semi-algebraic function is sub-analytic [1, 8]. For our problem in (6), $\mathcal{L}(\mathbf{U}, \mathbf{V}, b)$ is a real analytic function, and $\mathcal{R}(\mathbf{U}, \mathbf{V})$ is a semi-algebraic function, because the Euclidean norm $\|\cdot\|_2$ is shown to be semi-algebraic in [1, 8]. Therefore, the sum $F(\mathbf{U}, \mathbf{V}, b) = \mathcal{L}(\mathbf{U}, \mathbf{V}, b) + \mathcal{R}(\mathbf{U}, \mathbf{V})$ is sub-analytic, so $F(\mathbf{U}, \mathbf{V}, b)$ satisfies the KL inequality.

We start our analysis from this Lemma 1.

Lemma 1. (Square summable $\|(\mathbf{U}^k, \mathbf{V}^k, b^k) - (\mathbf{U}^{k+1}, \mathbf{V}^{k+1}, b^{k+1})\|_F$)

Let F be continuous in $\text{dom}(F)$ and $\inf_{(\mathbf{U}, \mathbf{V}, b) \in \text{dom}(F)} F(\mathbf{U}, \mathbf{V}, b) > -\infty$. Let the problem (6) have a Nash point, which is a block coordinate-wise minimizer. Moreover, if there exist constants $0 < \ell_u \leq L_u < \infty$ and $0 < \ell_v \leq L_v < \infty$ such that $\nabla_{\mathbf{U}}\mathcal{L}(\mathbf{U}, \mathbf{V}, b)$ and $\nabla_{\mathbf{V}}\mathcal{L}(\mathbf{U}, \mathbf{V}, b)$ are Lipschitz continuous, and parameters L_u and L_v follow $\ell_u < L_u^{k-1} \leq L_u$ and $\ell_v < L_v^{k-1} \leq L_v$, respectively, and $\mathcal{L}(\mathbf{U}^k, \mathbf{V}, b) \leq \mathcal{L}(\hat{\mathbf{U}}^{k-1}, \mathbf{V}, b) + \langle \nabla_{\mathbf{U}}\mathcal{L}(\hat{\mathbf{U}}^{k-1}, \mathbf{V}, b), \mathbf{U}^k - \hat{\mathbf{U}}^{k-1} \rangle + \frac{L_u^{k-1}}{2} \|\mathbf{U}^k - \hat{\mathbf{U}}^{k-1}\|_F^2$ and $\mathcal{L}(\mathbf{U}, \mathbf{V}^k, b) \leq \mathcal{L}(\mathbf{U}, \hat{\mathbf{V}}^{k-1}, b) + \langle \nabla_{\mathbf{V}}\mathcal{L}(\mathbf{U}, \hat{\mathbf{V}}^{k-1}, b), \mathbf{V}^k - \hat{\mathbf{V}}^{k-1} \rangle + \frac{L_v^{k-1}}{2} \|\mathbf{V}^k - \hat{\mathbf{V}}^{k-1}\|_F^2$ where $\hat{\mathbf{U}}^{k-1} = \mathbf{U}^{k-1} + \omega^{k-1}(\mathbf{U}^{k-1} - \mathbf{U}^{k-2})$ and $\hat{\mathbf{V}}^{k-1} = \mathbf{V}^{k-1} + \kappa^{k-1}(\mathbf{V}^{k-1} - \mathbf{V}^{k-2})$, which are extrapolated points.

Let $\{\mathbf{U}^k, \mathbf{V}^k, b^k\}$ be the sequence generated by the proposed BCPD algorithm with $0 \leq \omega^{k-1} \leq \delta_\omega \sqrt{\frac{L_u^{k-2}}{L_u^{k-1}}}$ and $0 \leq \kappa^{k-1} \leq \delta_\kappa \sqrt{\frac{L_v^{k-2}}{L_v^{k-1}}}$ for $\delta_\omega < 1$ and $\delta_\kappa < 1$, respectively. Then, $\sum_{k=0}^{\infty} \|(\mathbf{U}^k, \mathbf{V}^k, b^k) - (\mathbf{U}^{k+1}, \mathbf{V}^{k+1}, b^{k+1})\|_F^2 < \infty$ where $\|(\mathbf{U}, \mathbf{V}, b)\|_F = \sqrt{\|\mathbf{U}\|_F^2 + \|\mathbf{V}\|_F^2 + b^2}$.

Proof. Let $F(\mathbf{U}^k, \mathbf{V}^k, b^k) = \mathcal{L}(\mathbf{U}^k, \mathbf{V}^k, b^k) + \mathcal{R}(\mathbf{U}^k, \mathbf{V}^k)$ be the value of the objective function in (6) at $(\mathbf{U}^k, \mathbf{V}^k, b^k)$. Then we have

$$\begin{aligned}
F(\mathbf{U}^{k-1}, \mathbf{V}^k, b^k) - F(\mathbf{U}^k, \mathbf{V}^k, b^k) &\geq \frac{L_u^{k-1}}{2} \|\hat{\mathbf{U}}^{k-1} - \mathbf{U}^k\|_F^2 + L_u^{k-1} \langle \hat{\mathbf{U}}^{k-1} - \mathbf{U}^{k-1}, \mathbf{U}^k - \hat{\mathbf{U}}^{k-1} \rangle \\
&= \frac{L_u^{k-1}}{2} \|\mathbf{U}^{k-1} - \mathbf{U}^k\|_F^2 - \frac{L_u^{k-1}}{2} (\omega^{k-1})^2 \|\mathbf{U}^{k-2} - \mathbf{U}^{k-1}\|_F^2 \\
&\geq \frac{L_u^{k-1}}{2} \|\mathbf{U}^{k-1} - \mathbf{U}^k\|_F^2 - \frac{L_u^{k-2}}{2} \delta_\omega^2 \|\mathbf{U}^{k-2} - \mathbf{U}^{k-1}\|_F^2,
\end{aligned}$$

where in the first inequality we used the fact that if $f_1(\mathbf{x}^*) \leq f_1(\mathbf{y}) + \langle \nabla f_1(\mathbf{y}), \mathbf{x}^* - \mathbf{y} \rangle + \frac{L}{2} \|\mathbf{x}^* - \mathbf{y}\|^2$, then $f(\mathbf{x}) - f(\mathbf{x}^*) \geq \frac{L}{2} \|\mathbf{x}^* - \mathbf{y}\|^2 + L \langle \mathbf{y} - \mathbf{x}, \mathbf{x}^* - \mathbf{y} \rangle$ for any $\mathbf{x} \in \mathcal{X}$. Note that $f_1(\mathbf{x})$ and $f_2(\mathbf{x})$ are two convex functions defined on the convex set \mathcal{X} , $f_1(\mathbf{x})$ is differentiable, $f(\mathbf{x}) = f_1(\mathbf{x}) + f_2(\mathbf{x})$, and $\mathbf{x}^* = \operatorname{argmin}_{\mathbf{x} \in \mathcal{X}} \langle \nabla f_1(\mathbf{x}), \mathbf{x} - \mathbf{y} \rangle + \frac{L}{2} \|\mathbf{x} - \mathbf{y}\|^2 + f_2(\mathbf{x})$. More details can be found in [8]. Set $\mathbf{x} = \mathbf{U}^{k-1}$, $\mathbf{x}^* = \mathbf{U}^k$, and $\mathbf{y} = \hat{\mathbf{U}}^{k-1}$. Therefore, we have

$$\begin{aligned}
F(\mathbf{U}^{k-1}, \mathbf{V}^{k-1}, b^{k-1}) - F(\mathbf{U}^k, \mathbf{V}^k, b^k) &\geq F(\mathbf{U}^{k-1}, \mathbf{V}^k, b^k) - F(\mathbf{U}^k, \mathbf{V}^k, b^k) \\
&\quad + F(\mathbf{U}^k, \mathbf{V}^{k-1}, b^k) - F(\mathbf{U}^k, \mathbf{V}^k, b^k) \\
&\geq \left\{ \frac{L_u^{k-1}}{2} \|\mathbf{U}^{k-1} - \mathbf{U}^k\|_F^2 - \frac{L_u^{k-2}}{2} \delta_\omega^2 \|\mathbf{U}^{k-2} - \mathbf{U}^{k-1}\|_F^2 \right. \\
&\quad \left. + \frac{L_v^{k-1}}{2} \|\mathbf{V}^{k-1} - \mathbf{V}^k\|_F^2 - \frac{L_v^{k-2}}{2} \delta_\kappa^2 \|\mathbf{V}^{k-2} - \mathbf{V}^{k-1}\|_F^2 \right\}.
\end{aligned}$$

Then, we sum up the above inequality over k from 1 to K , we have

$$\begin{aligned}
F(\mathbf{U}^0, \mathbf{V}^0, b^0) - F(\mathbf{U}^K, \mathbf{V}^K, b^K) &\geq \sum_{k=1}^K \left\{ \frac{L_u^{k-1}}{2} \|\mathbf{U}^{k-1} - \mathbf{U}^k\|_F^2 - \frac{L_u^{k-2}}{2} \delta_\omega^2 \|\mathbf{U}^{k-2} - \mathbf{U}^{k-1}\|_F^2 \right. \\
&\quad \left. + \frac{L_v^{k-1}}{2} \|\mathbf{V}^{k-1} - \mathbf{V}^k\|_F^2 - \frac{L_v^{k-2}}{2} \delta_\kappa^2 \|\mathbf{V}^{k-2} - \mathbf{V}^{k-1}\|_F^2 \right\} \\
&\geq \sum_{k=1}^K \left\{ \frac{(1 - \delta_\omega^2) L_u^{k-1}}{2} \|\mathbf{U}^{k-1} - \mathbf{U}^k\|_F^2 \right. \\
&\quad \left. + \frac{(1 - \delta_\kappa^2) L_v^{k-1}}{2} \|\mathbf{V}^{k-1} - \mathbf{V}^k\|_F^2 \right\} \\
&\geq \sum_{k=1}^K \frac{(1 - \delta_\omega^2)(1 - \delta_\kappa^2) \ell_u \ell_v}{2} \|(\mathbf{U}^{k-1}, \mathbf{V}^{k-1}, b^{k-1}) - (\mathbf{U}^k, \mathbf{V}^k, b^k)\|_F^2.
\end{aligned}$$

Since F is bounded, the proof is done by taking $K \rightarrow \infty$. \square

For our problem, we can see that $F(\mathbf{U}^k, \mathbf{V}, b)$ and $F(\mathbf{U}, \mathbf{V}^k, b)$ are strictly less than $F(\mathbf{U}^{k-1}, \mathbf{V}, b)$ and $F(\mathbf{U}, \mathbf{V}^{k-1}, b)$, respectively as long as $\mathbf{U}^k \neq \mathbf{U}^{k-1}$ and $\mathbf{V}^k \neq \mathbf{V}^{k-1}$, since the objective function decrease at least $\frac{L_u^{k-1}}{2} \|\mathbf{U}^k - \mathbf{U}^{k-1}\|_F^2$ and $\frac{L_v^{k-1}}{2} \|\mathbf{V}^k - \mathbf{V}^{k-1}\|_F^2$, respectively when $\hat{\mathbf{U}}^{k-1} = \mathbf{U}^{k-1}$ and $\hat{\mathbf{V}}^{k-1} = \mathbf{V}^{k-1}$. Hence, if $\mathbf{U}^{k_0} = \mathbf{U}^{k_0-1}$ and $\mathbf{V}^{k_0} = \mathbf{V}^{k_0-1}$ for some k_0 , then $F(\mathbf{U}^k, \mathbf{V}, b) = F(\mathbf{U}^{k_0}, \mathbf{V}, b)$, $F(\mathbf{U}, \mathbf{V}^k, b) = F(\mathbf{U}, \mathbf{V}^{k_0}, b)$, $\mathbf{U}^k = \mathbf{U}^{k_0}$, and $\mathbf{V}^k = \mathbf{V}^{k_0}$ for all $k \geq k_0$, respectively.

Lemma 2.

Let $\{\mathbf{U}^k, \mathbf{V}^k, b^k\}$ be the sequence generated by the proposed BCPD algorithm with $L_u^k \geq L_u^{k-1}$, $L_v^k \geq L_v^{k-1}$, $\omega^k \leq \delta_\omega \sqrt{\frac{L_u^{k-1}}{L_u^k}}$, and $\kappa^k \leq \delta_\kappa \sqrt{\frac{L_v^{k-1}}{L_v^k}}$ for $\delta_\omega < 1$ and $\delta_\kappa < 1$, respectively. Note that our problem satisfies three conditions as below:

Condition 1. $\nabla_{\mathbf{U}}\mathcal{L}(\mathbf{U}, \mathbf{V}, b)$ and $\nabla_{\mathbf{V}}\mathcal{L}(\mathbf{U}, \mathbf{V}, b)$ are Lipschitz continuous on any bounded set.

Condition 2. F satisfies the KL inequality at $(\bar{\mathbf{U}}, \bar{\mathbf{V}}, \bar{b})$.

Condition 3. $(\mathbf{U}^0, \mathbf{V}^0, b^0)$ is sufficiently close to $(\bar{\mathbf{U}}, \bar{\mathbf{V}}, \bar{b})$, and $F(\mathbf{U}^k, \mathbf{V}^k, b^k) > F(\bar{\mathbf{U}}, \bar{\mathbf{V}}, \bar{b})$ for $k \geq 0$. Then, there is some $\mathcal{B} \subset \mathcal{U} \cap \text{dom}(\partial\varphi)$ with $\varphi = F$ such that $\{\mathbf{U}^k, \mathbf{V}^k, b^k\} \subset \mathcal{B}$ and $\{\mathbf{U}^k, \mathbf{V}^k, b^k\}$ converges to a point in \mathcal{B} .

Theorem. (Global Convergence)

Under the conditions 1, 2, 3 and that a sequence $\{\mathbf{U}^k, \mathbf{V}^k, b^k\}$ have a finite limit point $(\bar{\mathbf{U}}, \bar{\mathbf{V}}, \bar{b})$ where F satisfies the KL inequality, the sequence $\{\mathbf{U}^k, \mathbf{V}^k, b^k\}$ converges to $(\bar{\mathbf{U}}, \bar{\mathbf{V}}, \bar{b})$, which is a critical point of (6).

Proof. Note that $F(\mathbf{U}^k, \mathbf{V}^k, b^k)$ is monotonically nonincreasing and converges to $F(\bar{\mathbf{U}}, \bar{\mathbf{V}}, \bar{b})$. If $F(\mathbf{U}^{k_0}, \mathbf{V}^{k_0}, b^{k_0}) = F(\bar{\mathbf{U}}, \bar{\mathbf{V}}, \bar{b})$ at some k_0 , then $(\mathbf{U}^k, \mathbf{V}^k, b^k) = (\mathbf{U}^{k_0}, \mathbf{V}^{k_0}, b^{k_0}) = (\bar{\mathbf{U}}, \bar{\mathbf{V}}, \bar{b})$ for all $k \geq k_0$. On the other hand, consider $F(\mathbf{U}^k, \mathbf{V}^k, b^k) > F(\bar{\mathbf{U}}, \bar{\mathbf{V}}, \bar{b})$ for all $k \geq 0$. Since $(\bar{\mathbf{U}}, \bar{\mathbf{V}}, \bar{b})$ is a limit point and $F(\mathbf{U}^k, \mathbf{V}^k, b^k) \rightarrow F(\bar{\mathbf{U}}, \bar{\mathbf{V}}, \bar{b})$, there must exist an integer k_0 such that $(\mathbf{U}^{k_0}, \mathbf{V}^{k_0}, b^{k_0})$ is sufficiently close to $(\bar{\mathbf{U}}, \bar{\mathbf{V}}, \bar{b})$ according to Lemma 2. Hence, the entire sequence $\{\mathbf{U}^k, \mathbf{V}^k, b^k\}$ converges. Since $(\bar{\mathbf{U}}, \bar{\mathbf{V}}, \bar{b})$ is a limit point of $\{\mathbf{U}^k, \mathbf{V}^k, b^k\}$, we have $(\mathbf{U}^k, \mathbf{V}^k, b^k) \rightarrow (\bar{\mathbf{U}}, \bar{\mathbf{V}}, \bar{b})$. \square

References

- [1] Bocknak, L., Coste, M., and Roy, M.F. (1998), Real algebraic geometry. **36**, Springer Verlag.
- [2] Bolte, J., Daniilidis, A., and Lewis, A. (2007), The Lojasiewicz inequality for nonsmooth subanalytic functions with applications to subgradient dynamical systems. *SIAM Journal on Optimization*, **17**, pp.1205-1223.
- [3] Boyd, S., Vandenberghe L. (2004), Convex optimization. *Cambridge University Press*.
- [4] Tibshirani, R. (1996), Regression shrinkage and selection via the Lasso. *Journal of the Royal Statistical Society, Series B*, **58**(1), pp.267-288.
- [5] Chen, X., Aravkin, A., and Martin, D. (2018), Generalized linear model for gamma distributed variables via elastic net regularization. arXiv:1804.07780.
- [6] Lin, Q., Lu, Z., and Xiao, L. (2015), An accelerated randomized proximal coordinate gradient method and its application to regularized empirical risk minimization. *SIAM Journal on Optimization*, **25**(4), pp.2244-2273.
- [7] Shi, J., Xu, Y., Baraniuk, R.G. (2014), Sparse bilinear logistic regression. arXiv:1404.4104.
- [8] Xu, Y., and Yin, W. (2013). A block coordinate descent method for regularized multiconvex optimization with applications to nonnegative tensor factorization and completion. *SIAM Journal on imaging sciences*, **6**(3), pp.1758-1789.
- [9] Yuan, M, Lin, Y. (2007), Model selection and estimation in regression with grouped variables. *Journal of the Royal Statistical Society, Series B*, **68**(1), pp.49-67.